# Consideration of SLM additive manufacturing supports on the stability of flexible structures in finish milling

Paul Didier, Gael Le Coz, Guillaume Robin, Paul Lohmuller, Boris Piotrowski, Abdelhadi Moufki, Pascal Laheurte

# Consideration of SLM additive manufacturing supports on the stability of flexible structures in finish milling

P. Didier[1], G. Le Coz*[1], G. Robin[1], P. Lohmuller[1], B. Piotrowski[1], A. Moufki[1], P. Laheurte[1]

[1] Université de Lorraine, CNRS, Arts et Métiers ParisTech, LEM3, F-57000 Metz, France

Abstract:

The supports in additive manufacturing can be used in an innovative way by being considered as supports for machining operation. This innovative use of manufacturing supports can facilitate the finishing of functional thin structures. But the flexible global workpiece-supports system can potentially cause vibrations during the machining operation. This can cause irregular surfaces with bad quality.

This study highlights the importance of additively manufactured support structures on the stability of Ti-6Al-4V parts milling by using supports as a machining fixture. Nowadays, the control of the support stiffness and mechanical properties is not proposed by specific AM software. A way to develop a numerical method to optimize the post-processing of additive manufacturing parts is to use specific lattice structures as supports. Indeed, by adjusting the topology and the beam diameter of lattices, the relative stiffness and the relative density of the global structure can be controlled. The objective of this study is to show that the stiffness of the manufacturing supports is crucial for the machining operation.

To validate this concept, milling tests are proceeded on thin-walled plates produced by Selective Laser Melting (SLM) using defined finish milling cutting conditions. Three types of results are obtained: cutting forces signals, displacements and surface qualities by confocal microscopy. The study reveals that milling can induces chatters. Also, surface qualities and dimensional deviations depend on the support choice.

The control of mechanical properties of support structures appears to be a good way to favor machining operation of flexible and thin-walled structures. Topology and dimensional parameters of supports have to be considered in preliminary design steps of the additive manufacturing digital chain.

Keywords: Selective Laser Melting (SLM); Additive Manufacturing support; machining.

## 1. Introduction

The growing interest in Additive Manufacturing (AM) processes and particularly in the Selective Laser Melting (SLM) technology resulted in the development of the associated techniques: “design for additive manufacturing”. This offers new opportunities and considerations despite new constraints [1]. The possibilities offered of 3D printing technology make it possible to redesign products by taking advantage of these new processes [2]. For example, in the biomedical field, it is possible to manufacture custom-made implants and prosthesis which perfectly adapt to bone anatomy [3]. Automotive, aeronautical and aerospace industries are particularly attracted by the freedom of shapes, allowing the manufacturing of topologically optimized macro-structures [4] and complex beam network, such as lattices structures [5]. Numerical approaches of topological optimization allow to

determine the optimal distribution of material in a defined volume subjected to specific loads for the lightening of the structure. [6]. All these new possibilities lead to complex geometries and thin-walled structures.

Additive manufacturing technologies also impose various constraints [1, 7]. For instance, the process to obtain powder for SLM technology is expensive and thus the achievable alloy compositions are limited. The control of the process allows very low porosity rates but leads to anisotropic mechanical properties and irregular surface roughness that are strongly dependent on the orientation of the parts on the substrate [8, 9]. Residual stresses related to rapid cooling induce geometrical deviations [10]. During the manufacturing processes, manufacturing supports are always used to limit strains by strengthening the overall structure and favoring a better heat diffusion during manufacturing [11]. However, support structures have to be removed afterward. This may take time and require manual operations causing topological defects. These defects further aggravate roughness defects.

Although additive manufacturing process makes it possible to approach the near-net shape of the product, finishing operations by chemical [12], mechanical [13] or laser treatment [14] are necessary. For some surfaces, accurate dimensional qualities are required and thus finishing by milling or grinding is necessary [15]. These treatments have already been integrated by some companies in their hybrid machining center offering additive manufacturing and milling possibilities [16], where material deposition and machining operation are performed in the same place. In the case of SLM process, the hybrid solutions are more complicated due to the powder deposition. Thus, the complementarity between the additive and the subtractive machines must be investigated and the repositioning methods for machining of the produced part should be considered.

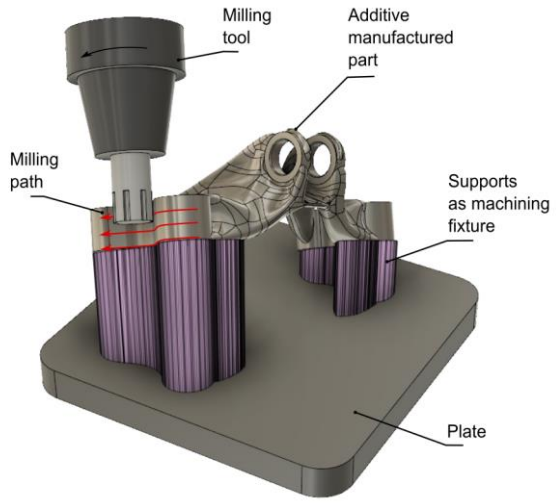


*Figure 1 – Machining operation of an additive manufactured part with consideration of supports as a machining fixture.*

The concept investigated in this study is the following: considering the machining operation by milling, it is possible to consider the supports no longer as a constraint, but as an opportunity, as a customized machining fixture. The support structures are preserved in order to perform post-processing on specific surfaces, see Figure 1. This approach allows a gain of operations to obtain finished functional surfaces. This strategy eliminates the need to develop a specific clamp for a unique, custom-made, complex-shaped part. Its potential leads to the cost-effectiveness of production where post-processing is still considered to be artisanal. To achieve such a goal, several considerations need taking into account. The first technical aspect that should be considered is the appropriate positioning and the orientation of the printed part in order to make the considered surfaces accessible to the cutting tool. The second is the geometry and the stiffness heterogeneity of the global manufacturing part, including

the manufacturing supports and the workpiece. These factors are unfavorable for the milling, due to the bending of the flexible part, and thus vibrations can appear between the tool and the part [17]. This situation generates dimensional deviations and low surface quality [18]. It is then necessary to understand the vibratory phenomenon in order to anticipate, control and limit it by optimizing cutting speed and material removal rate [19-21]. Although the printed part is not adaptable because of the function that it was designed for, the supports can be optimized. They can be used to modify the mechanical properties of the part that supports the overall system, as sacrificial structures to increase the stiffness [22] or a mass damper to adjust the eigenfrequency of the structure [23]. However, in the digital chain dedicated to additive manufacturing, supports are principally designed to build an unsupported overhang structure or to limit part distortion. Considering the literature review of Plocher and Panesar [24], there is no previous work including the support structure optimization taking into account all the mechanical loads applied during the post-processing. Indeed, the control of their equivalent stiffness and their equivalent mechanical properties is not considered. In the same way as Hussein et al. [11] proposes to use lattice structures as supports to minimize the lasering time. A novel approach is to consider lattices structures as supports with the ability to control the mechanical properties of the overall additive manufacturing part, with the objective of post-processing the surfaces by milling.

Thus, the present work is proposed to use lattices structures as custom-made supports directly manufactured during the process. This study highlights the influence of support stiffness on the milling operation and its effect on the quality of the finished surfaces. Side milling tests are carried out on plate samples and their manufacturing supports. Support structures with different stiffnesses are compared, using different geometrical and sizes of support structures. Cutting forces and displacements are measured using a dynamometric plate and a laser vibrometer. A correlation to the surface quality is presented.

## 2. Material and methods

### 2.1. Geometry and SLM additive manufacturing of the samples

Differences of stability in milling and potential vibration problems are highlighted by the design of adequate SLM samples. In the previous studies about chatters when machining, milling instability directly resulted from the thin thickness of thin-walled plates. Thevenot et al. [19] milled a 1-millimeter thin wall of steel plate (S235) and Seguy et al. [18] worked with a 2017 aluminum alloy workpiece with 3 mm in thickness and 20 mm in height.

In the present work, the system is composed of two parts of Ti-6A-l4V. The main deflection of the plates is due to the open geometry of the supports and their low stiffness. Samples with two subparts are considered and the geometry of the samples is presented in Figure 2. These two parts are manufactured on a third block (unrepresented) that allows the clamping of the samples in the machining center and ensures an embedment of the samples at the base of the support-plate system. The upper rectangular-shaped plate, 3 mm thickness ($l_1$), 9 mm high ($l_2$) and 9 mm wide ($l_4$), is the subpart to be finished by machining. The lower part of the samples corresponds to the manufacturing support. Its thickness is equal to ($l_1$) and the height ($l_3$) to 4.5 mm. As the geometrical shape is fixed, the sample stiffness is controlled by the geometry and the architecture of the supports. Two families of structures are considered in this study to cover a large range of stiffness: structures directly exported from the SLM digital chain and lattices structures, as shown in Figure 2.

The first supports are obtained with the Magics® Materialise software, dedicated to the data preparation for SLM. The *Web* support is composed of various vertical walls, one crossing another at the center of the surface. The *Block* support consists of intersecting walls with diamond-shaped perforations. The second type of supports proposed are lattice structures, made by the repetition of an elementary unit-cell. By adjusting the topology and the beam diameter, the relative stiffness and the relative density of the global structure can be controlled and numerically implemented. These mechanical properties are essential to understand the dynamic phenomenon during milling. Indeed, with the control of the truss diameter and the unit-cell size, and thus the control of the relative density, it is possible to determine its Young's modulus [25]. Two structures, well known in the literature, are retained in this study: the *Diagonal* and the *Octet-truss* structure [26]. Two truss diameters are considered for each cell: 0.300 and 0.375 mm. The same global unit-cell dimension of 1.5x1.5x1.5 $mm^3$ are used and the same pattern repetition (6x2x3) in the x, y and z directions are used to define the global samples with fixed dimensions. For each structure, four samples are prepared, using the laser manufacturing parameters for the Ti-6Al-4V alloy (Power P = 200 W, laser speed v = 1650 mm/sec and hatching distance H = 80 µm).

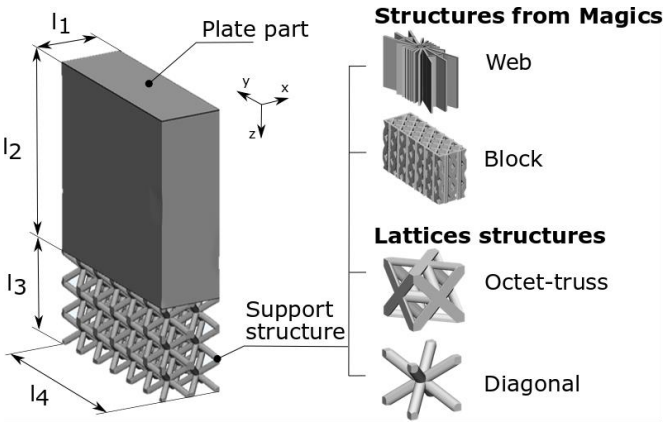


*Figure 2 - Geometry of the two types of sample: lattice structures and AM software structures*

## 2.2. Analysis of the first modal frequency

The sample is composed of two parts: the upper plate and the lower support that has the equivalent behavior of a bulk plate structure. Embedded in the base, the natural principal deformation is the flexion around the y-axis, as shown in Figure 2. As all the samples have the same external dimensions, they have the same first mode of vibration corresponding to the flexion around the y-axis. Since the natural frequencies of the plate increase with its rigidity, the stiffness of each sample is analyzed through the natural frequency of the first mode $f_1$.

An impact hammer allows us to determine the resonance frequency of the structure. The displacements are measured by a laser vibrometer. As there is no contact between the sensor and the workpiece, the measurement is not disturbed. The frequency range of the solicitation is from 1Hz to 10 000Hz. The laser is focused in the middle of the free end of the plate. A Fast Fourier Transformation (FFT) is performed to obtain the frequency content of the vibration signal. The first modal frequency is scattered with a lower value of 743 Hz for the *Diagonal* with 0.3 mm diameter to 6656 Hz for the *Block* sample, as given in Table 1. The dispersion is slightly increased for structures with 0.3 mm in diameter (8.21 %) from that for the structures with 0.375 mm in diameter (4.59 %). Indeed, at this scale, the geometrical defects due to the process are even more important with smaller diameters

[27]. Owing to the resolution, the reproducibility of the process is validated, particularly for the Magics® supports. The reproducibility of the process can be validated for all structures.

*Table 1 - Average of the first modal frequency of each structure and dispersion*

| Structure | $f_1$ (Hz) | Relative deviation (%) | Damping η |
|---|---|---|---|
| *Diagonal* with 0.300 mm diameter | 743 | 8.21 | 0.0024 |
| *Diagonal* with 0.375 mm diameter | 1459 | 4.59 | 0.0018 |
| *Octet-truss* with 0.300 mm diameter | 2780 | 5.52 | 0.0022 |
| *Octet-truss* with 0.375 mm diameter | 4601 | 2.04 | 0.0012 |
| *Block* | 6656 | 2.72 | 0.0018 |
| *Web* | 4551 | 1.14 | 0.0011 |

## 2.3. Experimental tests of finish milling

The peripheral finish milling of the plate (thin wall) is proceeded in a Roeders RXP200DS (3000 – 60000 rpm) 5 axis machining center, with an Erowa ITS50 clamping system. Side up milling operation is carried on with a TiAlN coated solid carbide tool, referenced as Belet 110-1. The tool has four teeth, a helix angle of 30° and a cutting angle between 8° and 10°. The diameter of the tool is 3 mm with a 6 mm diameter body at the end. It is assembled in a collet chuck system referenced as BIG New Baby Chuck. The samples defined previously are clamped on a dynamometric platform, Kisler 9256C, as shown in Figure 3 (a). It allows measuring the cutting forces in three directions in the three-dimensional space. A charge amplifier Kisler 5017B integrated with an acquisition system NI Daq and a Labview program enable the recording of the cutting force signals at a frequency of 10 kHz. The tool-machine framework is considered to be perfectly rigid compared with the workpiece which is considered flexible.

The displacements of the thin wall when machining are also measured with a laser vibrometer in the middle of the free end of the plate; the laser beam is represented Figure 3 (a). The side milling of the SLM plates is performed in finishing conditions of the conventionally produced Ti-6Al-4V alloy, with a cutting speed of 141 m/min, a feed per tooth ($f_z$) of 14 µm/th and an axial and radial depth of cut ($a_e$) of 1 and 0.2 mm, respectively, as seen in Figure 3 (b). It corresponds to a spindle speed (N) of 15000 rpm. Two milling passes are performed for each sample. The first pass can't be considered as constant, due to the initial surface state, including roughness and particles partially melted. The first pass can be considered as roughing. To obtain constant conditions, the presented displacements and cutting forces are related to the second pass, considered as finishing.

Surface topography is obtained after milling tests by confocal microscopy with a Leica DCM3D system. The associated software Leica Map facilitates the extraction of profiles and surfaces. These data provide Ra measurements calculated on 1 mm lengths in the same direction as the machining pass.

The topography of the surfaces can also be used to extract the difference in height between the machined surface and the rough surface.

Temporal evolution of the cutting forces, displacements and surface topographies obtained by confocal microscopy are evaluated at two different scales:

- at the global scale (all along the plate): the dynamic behavior of the structure, that depends on the solicitation position, especially at the extremities of the plate;
- at the local scale (tens of micrometers): the impact of each tooth on the structure.

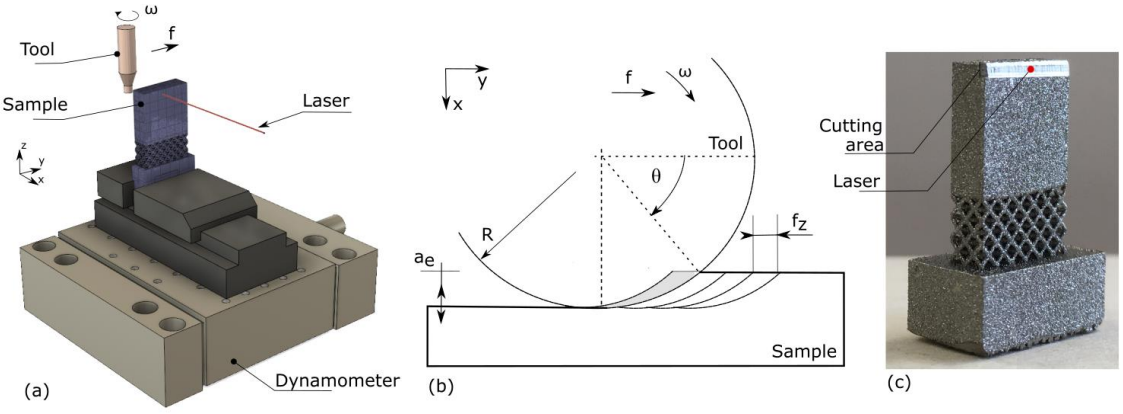


*Figure 3 - (a) Experimental procedure implemented, (b) Cutting schema of finishing pass and associated parameters and (c) Manufactured sample presenting the milling pass.*

## 3. Results

Table 2 summarizes the overall results for all structures. This takes into account the average amplitude of displacement and force on the two machining passes, the height between the machined surface and the rough surface (in confocal microscopy) and the roughness Ra. Only the *Diagonal* structure with 0.3 mm diameter did not allow the acquisition of all signals due to failure of the supports during the machining operation. Globally, the more rigid the structure is, the less the amplitude of its displacement is important and the higher the cutting effort. Thus, the removal of material is more important as indicated by the difference in height between the machined surface and the rough surface. Finally, the surface roughness is much smoother for more rigid structures.

In order to study more precisely the impact of the stiffness of the supports on the machining operation, three structures are studied more closely. The objective is to identify two milling regimes (stable or unstable) through two structures with far different stiffness: *Block* structure ($f_1$ = 6656 Hz) and *Octet-truss* structure with a 0.3 mm diameter ($f_1$ = 2780 Hz). They are compared to a third one with intermediate stiffness: *Octet-truss* with 0.375 mm diameter ($f_1$ = 4601 Hz).

*Table 2 - Summary of machining test results: displacement amplitude, cutting force, height difference between machined and rough surface and roughness Ra*

| Structure | f1 (Hz) | Average displacement amplitude (mm) | Average cutting force amplitude (N) | Minimum & maximum force (N) | Height difference: rough-machined surfaces (µm) | Ra (µm) |
|---|---|---|---|---|---|---|
| **Diagonal with 0.300 mm in diameter** | 743 | / | / | / | 35.5 | 5.09 |

| | | | | | | |
|---|---|---|---|---|---|---|
| **Diagonal with 0.375 mm diameter** | 1459 | 0.87 | 25.4 | 6.9<br>107.1 | 54 | 0.45 |
| **Octet-truss with 0.300 mm diameter** | 2780 | 0.70 | 37.9 | 17.3<br>72.7 | 64 | 0.38 |
| **Octet-truss with 0.375 mm diameter** | 4601 | 0.38 | 63.7 | 25.3<br>73.6 | 169.5 | 0.19 |
| **Block Magics** | 6656 | 0.31 | 83.1 | 98.3 | 283 | 0.11 |
| **Web Magics** | 4551 | 0.40 | 64.5 | 35.2<br>76.4 | 145.5 | 0.23 |

## 3.1. Displacement

The displacement at the global scale is firstly considered, see Figures 4 (a), (d) and (g). It shows that whatever the stiffness of the sample, the signal has the same aspect with a stable central area, composing the majority of the signal. At the beginning and at the end of the signal, edge effects are visible with different amplitudes compared with that at the stable central area. When the three plates are compared to each other, it can be seen that the more the plate is flexible, the higher the amplitude of the signal is. The same trend is observed for the edge effect.

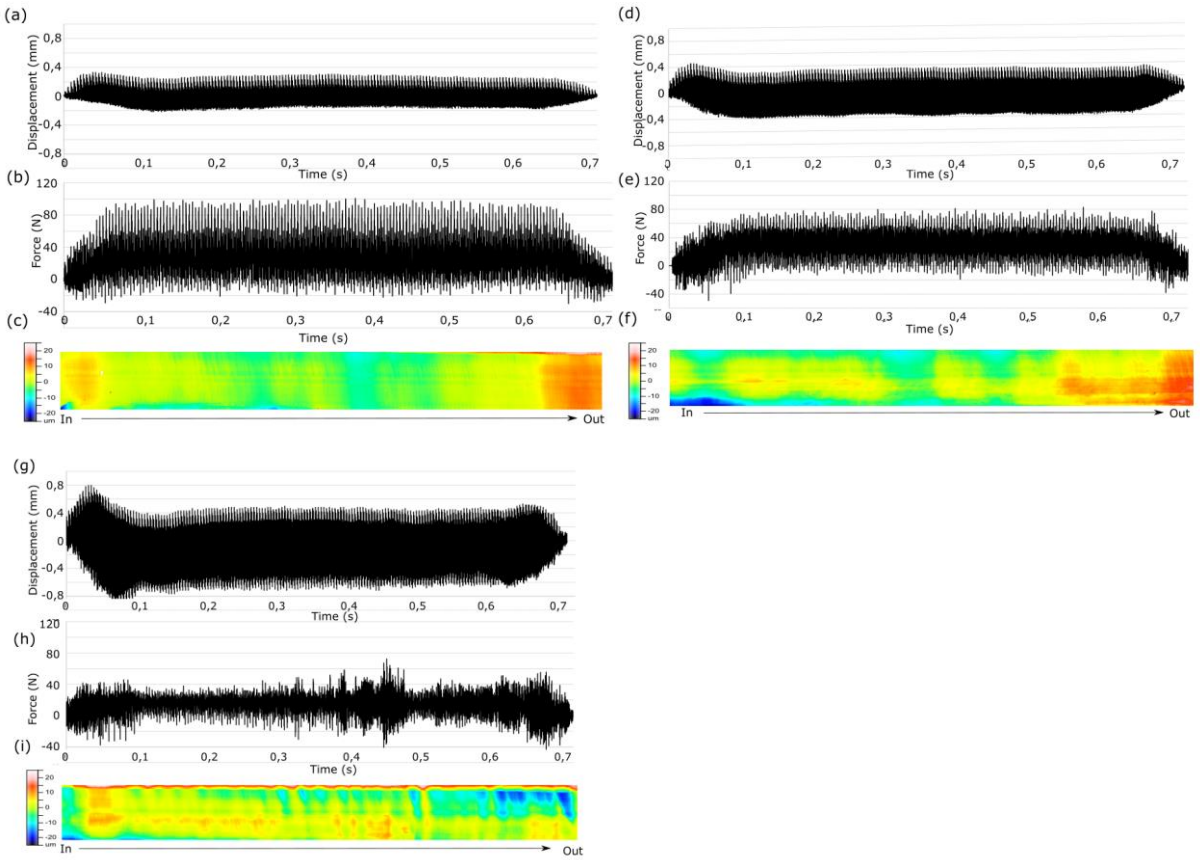


*Figure 4 - Normal displacements, normal cutting force and surface topography for the Block structure (a) (b) (c), the Octet-truss with a 0.375 diameter (d) (e) (f) and the Octet-truss with a 0.3 mm diameter structure (g) (h) (i) - Global scale*

Displacement is evaluated at the local scale and in the middle of the milling pass for three tool rotations, as shown in Figures 5 (a), (d) et (g). The impact of each tooth is clearly observed, with a period of 1 ms. Four impacts correspond to a tool rotation duration of 4 ms. Furthermore, the displacement imposed by each tooth is not equivalent and is decreasing with the four successive teeth, typical to a tool run out.

The signal of the higher stiffness plate (*Block*) presents a 0.2 ms phase without movement, equivalent to a 0.1 mm displacement, see Figure 5 (a). The *Octet-truss* structure with 0.375 mm diameter is more flexible, and the signal amplitude is higher and oscillates continuously from -0.35 to 0.35 mm, as seen in Figure 5 (d). At last the *Octet-truss* structure with 0.3 mm diameter is less rigid with a displacement oscillating between -0.6 and 0.35 mm, see Figure 5 (g).

### 3.2. Cutting forces

The displacement acquired with the laser interferometer in the normal direction of the plate is correlated with the normal cutting force in the same direction $F_x$. For the *Block* structure, the most part of the signal is stable, as seen in Figure 4 (b). Edge effect can be seen at the extremities marked by a limited force at the beginning and at the end of the milling. Moreover, as seen from the displacement, the edge effect is more marked for the less rigid structure with the more perturbed signal at the extremities. However, some irregularities and punctual instabilities, not observed on the displacement signal, are observed all along the *Octet-truss* with 0.3 mm diameter, as shown in Figure 4 (h). For the intermediate structure, the cutting force signal remains stable but with a lower amplitude than the *Block* structure, see Figure 4 (e). At the local scale, the impact of each tooth is clearly identified for the *Block* structure, as seen in Figure 5 (b). Due to a run out of the tool, an asymmetry between different teeth is observed, as seen on the displacement. It confirms the correlation between the two signals. Figure 5 (h) shows that for the flexible sample the impact of each tooth is hardly noticeable. In terms of the amplitude, the force signal decreases with the loss of the stiffness, both locally and globally.

### 3.3. Topography of surface

Figure 4 also presents the surface topography on all the cutting area, obtained by confocal microscopy. The surface quality appears completely different for the three samples. For the *Block* structure which is more rigid, the height variations all along the plate are small and of the order of 10 µm, see Figure 4 (c). This variation is due to the side effect, especially at the output of milling. Despite these edge effects, the global topography is regular. The surface quality of the *Octet-truss* with 0.375 mm diameter is less homogeneous than the *Block* structure as shown in Figure 4 (f). The topography of the *Octet-truss* with 0.3 mm diameter structure is even more irregular, see Figure 4 (i). The variation reaches 30 µm and the punctual vibrations seen on the cutting force signal are also observed on the surface. These observations are consistent with the determination of Ra roughnesses presented in Table 2.

At the local scale, the surface is evaluated in the middle of each plate, as presented in Figure 5. The profiles are extracted from a length of 0.5 mm. On the *Block* surface, the waviness due to the cutting is clearly visible, see Figure 5 (c). On the profile, the waviness period is averaged to be 56 µm. It corresponds to the feed rate per revolution. For the more rigid *Octet-truss* structure with 0.375 mm diameter, the periodic waves due to the cutting are less visible, but the surface quality is not significantly affected, see Figure 5 (f). The surface is considerably more degraded for the flexible Octet-truss structure with 0.3 mm diameter, where the irregularity of the cutting is evident, as seen in Figure 5 (i).

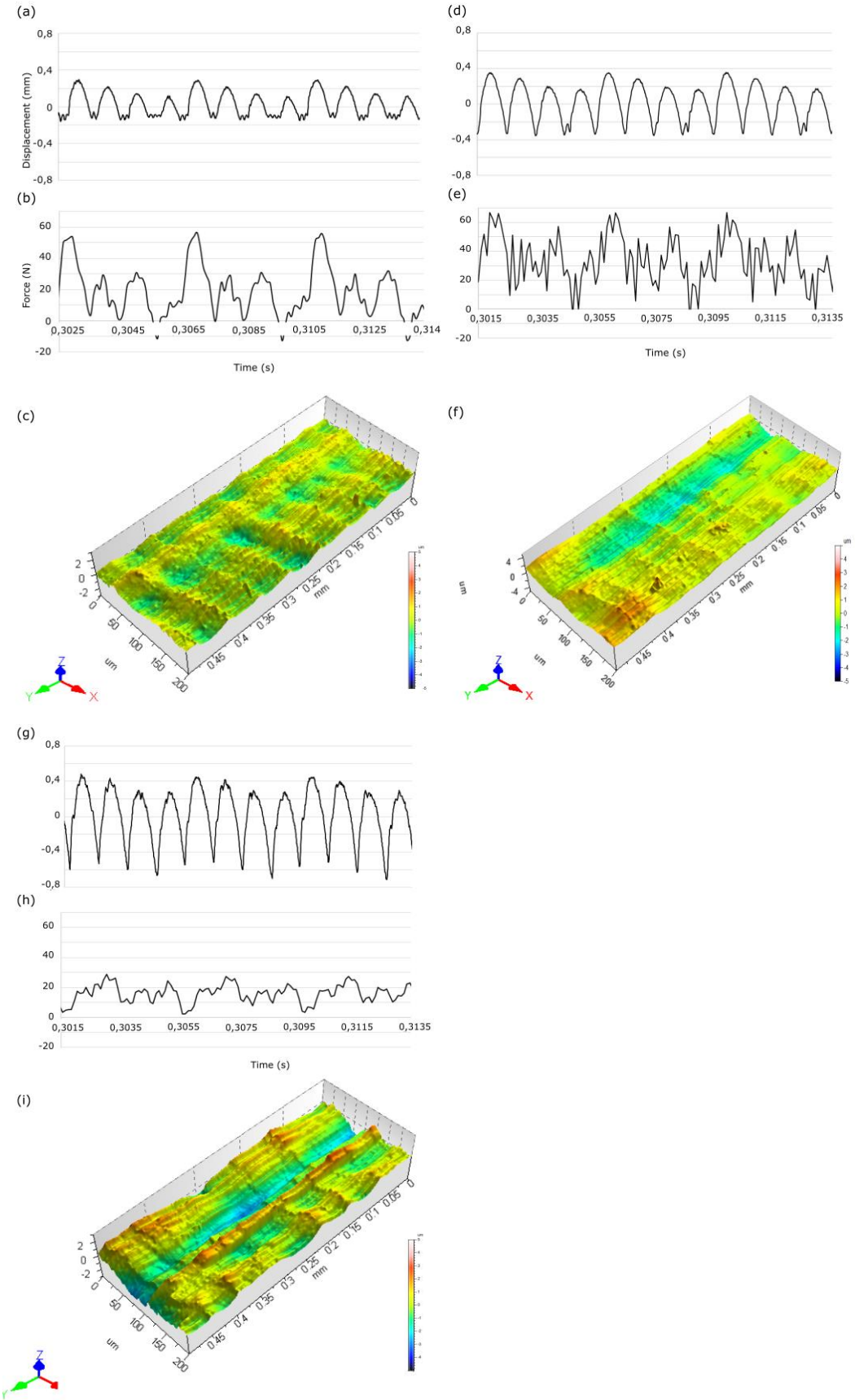


*Figure 5 - Normal displacements, normal cutting force and surface topography for the Block structure (a) (b) (c), the Octet-truss with a 0.375 diameter (d) (e) (f) and the Octet-truss with a 0.3 mm diameter structure (g) (h) (i) - Local scale*

## 4. Discussion

SLM process allows a near-net-shape product but some functional surfaces still need to be post-processed. This operation contracts additional costs and thinking for planning [28]. The novel approach, considering support as custom-made machining fixture for post-machining, answers to a step between additive process and subtractive milling. It leads to study the overall workpiece, including the plate and the support structure. Milling operation can induce chatters and poor surface quality, depending on the support choice but also of the cutting parameters. Previous works [18-20] propose to determine lobes stability when side milling. In the present study, authors limit the discussion and only focus on the effect of part stiffness.

A correlation can be established between the stiffness of the workpiece and the plate displacement in flexion. The more flexible the structure is, the greater its bending displacement. This trend is confirmed by the evolution of the average displacement (in the stable area) according to its first modal frequency, as seen in Figure 6. The curve shows a nonlinear increase of the average displacement with the decrease of $f_1$. This amplification can be explained by the growing proximity between $f_1$ and the excitation frequency of the tool tooth, corresponding to 1000 Hz. Nevertheless, the information obtained from the displacement signals is not sufficient to confirm the effective cutting of the material.

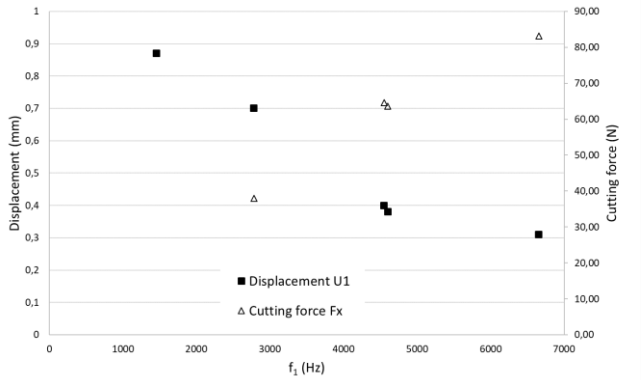


*Figure 6 - Evolution of the average displacement amplitude and cutting force according to the first modal frequency*

In contrary to the displacement signal, a decrease of the cutting force amplitude is observed with the loss of stiffness. The decreasing amplitude of the signal indicates a less effective cutting of the material for the least rigid structure. The more the plate is flexible, the larger its deflection is, and thus less material is cut by the tool. This non-cutting phenomenon is even more pronounced when the axial depth of cut is small. Indeed, in these cutting conditions, the scale of the deflection and the radial depth of cut ($a_e$) are the same. The previous tendencies are supported by the surface profiles, as shown in Figure 7. These data, acquired by confocal microscopy, demonstrate the difference of heights between the manufactured rough surface and the finished surface. After two passes of 0.2 mm, the height difference gap should theoretically be 0.4 mm. For the *Block* sample, the most rigid of all the studied structures, the real average total depth of cut is 0.3 mm. For the *Octet-truss* structure with 0.3 mm diameter, the difference does not exceed 0.1 mm. Thus, the deflection of the flexible parts has also considerably affected the cutting considering the dimensional expected results. The irregularities and singularities noted all along this flexible *Octet-truss* plate can indicate cutting instabilities due to vibratory problems. Indeed, the more flexible structures have a first modal frequency close the excitation frequency. Hence, vibration problems inducing irregular and bad cutting are more remarkable for these samples.

Other phenomena have also appeared during the machining of the plates. On the global displacement signals, edge effects are visible when the tool is cutting the extremities of the plate. When the

mechanical solicitation is positioned on the sides of the sample, the flexion is amplified, and the displacement at the solicited extremity is larger than the displacement at the center of the plate. This phenomenon is even more marked when the plate is flexible. Indeed, edge effects are often observed in side milling of thin-walled plates [19]. As mentioned previously, despite the laser is at the center of the plate, the perturbation is detectable and increases with the reduction of the stiffness of the structures. Moreover, an asymmetry between the teeth has been detected from cutting force and displacement signals, defined as a runout. It can be explained by a tiny manufacturing defect of the tool, especially observed in micro milling, where cutting tool depth of cut ($a_e$, f) is small. This phenomenon results in a regular waviness for the *Block* sample where the resultant surface is from the action of the most eccentric tooth, as shown in Figure 5 (a). For the *Octet-truss* with 0.3 mm diameter sample, the surface is more chaotic, and the milling waviness is not visible, as seen from Figure 5 (g). The trochoidal movement of the tool teeth is combined with the oscillation of the flexible plate which results in particularly degraded surface topography. This is due to the increasing deflection of the plate with the decreasing of the equivalent rigidity of the support structures. Hence, the final surface quality also depends on the architecture of the lattice structures.

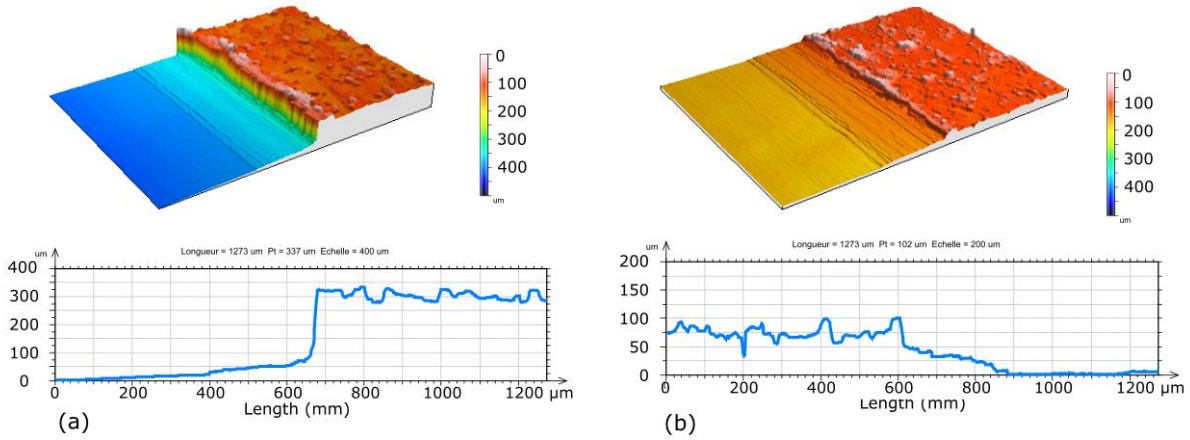


*Figure 7 - Profile between rough and cut surfaces for (a) Block structure and (b) Octet-truss 0.3 mm diameter structure, acquired by confocal microscopy*

The support structures made by AM, when they used as machining supports, have a major role on the final surface quality of the parts. Their equivalent stiffness, or more generally their mechanical property also allows the control of the final dimensions of the AM finished parts. Lattices structures, although less rigid than the *Block* structure, allow to adjust mechanical behavior of the global workpiece when submitted to the dynamic solicitation of the milling operation. Indeed, contrary to traditional supports designed to build overhang surface during the additive process, lattices structures stiffness can be controlled by a numerical method. For example, lattices structures can be submitted to simple procedure of numerical homogenization [29], replacing the complex support structure with a simplified geometry with equivalent mechanical properties. Considering the natural shape of the generative designed part, see Figure 1, the use of controlled supports really makes sense. They could allow the anticipation and the choice of the supports architecture, by analytical model [25] coupled with Finite Element Analysis of the part-support system. In that way, the process could be optimized to define support architecture and mass as a tuned mass damper. Moreover, sacrificial supports, not necessarily useful for AM, could be added to stabilize the peripheral milling of flexible parts, as used in other domains [22]. For example, additional lattice buttresses defined as sacrificial structures can temporarily increase the stiffness of part when milling interested surface before being removed.

Others possibilities exist with numerical tools and FEA modelization. In that way, a coupled analytical-numerical model of the cutting forces could help for the supports design basis [30, 31].

## 5. Conclusions

The study proposes a novel approach considering supports as a custom-made machining fixture for machining operation. To demonstrate the concept, experimental tests of finish milling have been done on plate structures on their supports, manufactured by SLM additive process. The equivalent stiffness of the overall workpiece varies with the geometry and architecture of the manufacturing supports. Lattice structures and supports from commercial SLM software were used to cover a large range of stiffness. Cutting forces, displacement and surface topology were measured. With two principal observations, the study highlights the importance of the choice of manufacturing supports in terms of stiffness on the milling of SLM workpiece:

- Even under finishing conditions, milling can induce chatters, depending on the support choice. The correlation between the plate displacement and the cutting forces confirms a more and more irregular and ineffective cutting with the loss of stiffness of the supports.
- Surface qualities and dimensional deviations depend on the support structures. Vibration phenomena amplify the cutting instability, especially for the most flexible structures, whose first modal frequency is close to the excitation frequency of the teethed tool.

The actual associated digital chain does not allow optimal control of the mechanical behavior of the supports. This makes the lattice structures an excellent candidate for numerical analysis of manufacturing supports in the way to use it as custom-made machining supports. Indeed, they allow a choice of equivalent stiffness and mechanical properties. This study also opens up the possibility of numerically predicting the dynamic behavior of the part-support system in order to include the finishing operations in the design of additive manufacturing.

## References:


[1] Thompson, M. K., Moroni, G., Vaneker, T., Fadel, G., Campbell, R. I., Gibson, I., & Martina, F. (2016). Design for Additive Manufacturing: Trends, opportunities, considerations, and constraints. CIRP annals, 65(2), 737-760.

[2] Gibson, I., Rosen, D. W., & Stucker, B. (2014). Additive manufacturing technologies (Vol. 17). New York: Springer.

[3] Didier, P., Piotrowski, B., Fischer, M., & Laheurte, P. (2017). Mechanical stability of custom-made implants: Numerical study of anatomical device and low elastic Young's modulus alloy. Materials Science and Engineering: C, 74, 399-409.

[4] Saadlaoui, Y., Milan, J. L., Rossi, J. M., & Chabrand, P. (2017). Topology optimization and additive manufacturing: Comparison of conception methods using industrial codes. Journal of Manufacturing Systems, 43, 178-186.

[5] Zhang, X. Z., Leary, M., Tang, H. P., Song, T., & Qian, M. (2018). Selective electron beam manufactured Ti-6Al-4V lattice structures for orthopedic implant applications: Current status and outstanding challenges. Current Opinion in Solid State and Materials Science, 22(3), 75-99.

[6] Bendsoe, M. P., & Sigmund, O. (2013). Topology optimization: theory, methods, and applications. Springer Science & Business Media.

[7] Hague, R., Campbell, I., & Dickens, P. (2003). Implications on design of rapid manufacturing. Proceedings of the Institution of Mechanical Engineers, Part C: Journal of Mechanical Engineering Science, 217(1), 25-30.

[8] Simonelli, M., Tse, Y. Y., & Tuck, C. (2014). Effect of the build orientation on the mechanical properties and fracture modes of SLM Ti–6Al–4V. Materials Science and Engineering: A, 616, 1-11.

[9] Leary, M. (2017). Surface roughness optimisation for selective laser melting (SLM): accommodating relevant and irrelevant surfaces. In Laser Additive Manufacturing (pp. 99-118). Woodhead Publishing.

[10] Mugwagwa, L., Dimitrov, D., Matope, S., & Yadroitsev, I. (2018). Influence of process parameters on residual stress related distortions in selective laser melting. Procedia Manufacturing, 21, 92-99.

[11] Hussein, A., Hao, L., Yan, C., Everson, R., & Young, P. (2013). Advanced lattice support structures for metal additive manufacturing. Journal of Materials Processing Technology, 213(7), 1019-1026.

[12] Baicheng, Z., Xiaohua, L., Jiaming, B., Junfeng, G., Pan, W., Chen-nan, S., & Jun, W. (2017). Study of selective laser melting (SLM) Inconel 718 part surface improvement by electrochemical polishing. Materials & Design, 116, 531-537.

[13] Salvatore, F., Grange, F., Kaminski, R., Claudin, C., Kermouche, G., Rech, J., & Texier, A. (2017). Experimental and numerical study of media action during tribofinishing in the case of SLM titanium parts. Procedia CIRP, 58, 451-456.

[14] Yung, K. C., Xiao, T. Y., Choy, H. S., Wang, W. J., & Cai, Z. X. (2018). Laser polishing of additive manufactured CoCr alloy components with complex surface geometry. Journal of Materials Processing Technology, 262, 53-64.

[15] Brinksmeier, E., Levy, G., Meyer, D., & Spierings, A. B. (2010). Surface integrity of selective-laser-melted components. CIRP annals, 59(1), 601-606.

[16] Stavropoulos, P., Foteinopoulos, P., Papacharalampopoulos, A., & Bikas, H. (2018). Addressing the challenges for the industrial application of additive manufacturing: Towards a hybrid solution. International Journal of Lightweight Materials and Manufacture, 1(3), 157-168.

[17] Michalik, P., Zajac, J., Hatala, M., Mital, D., & Fecova, V. (2014). Monitoring surface roughness of thin-walled components from steel C45 machining down and up milling. Measurement, 58, 416-428.

[18] Seguy, S., Dessein, G., & Arnaud, L. (2008). Surface roughness variation of thin wall milling, related to modal interactions. International Journal of Machine Tools and Manufacture, 48(3-4), 261-274.

[19] Thevenot, V., Arnaud, L., Dessein, G., & Cazenave-Larroche, G. (2006). Integration of dynamic behaviour variations in the stability lobes method: 3D lobes construction and application to thin-walled structure milling. The International Journal of Advanced Manufacturing Technology, 27(7-8), 638-644.

[20] Altintaş, Y., & Budak, E. (1995). Analytical prediction of stability lobes in milling. CIRP annals, 44(1), 357-362.

[21] Denkena, B., & Schmidt, C. (2007). Experimental investigation and simulation of machining thin-walled workpieces. Production engineering, 1(4), 343-350.

[22] Smith, S., Wilhelm, R., Dutterer, B., Cherukuri, H., & Goel, G. (2012). Sacrificial structure preforms for thin part machining. CIRP annals, 61(1), 379-382.

[23] Kolluru, K., Axinte, D., & Becker, A. (2013). A solution for minimising vibrations in milling of thin walled casings by applying dampers to workpiece surface. CIRP Annals, 62(1), 415-418.

[24] Plocher, J., & Panesar, A. (2019). Review on design and structural optimisation in additive manufacturing: Towards next-generation lightweight structures. Materials & Design, 183, 108164.

[25] Favre, J., Lohmuller, P., Piotrowski, B., Kenzari, S., Laheurte, P., & Meraghni, F. (2018). A continuous crystallographic approach to generate cubic lattices and its effect on relative stiffness of architectured materials. Additive Manufacturing, 21, 359-368.

[26] Deshpande, V. S., Fleck, N. A., & Ashby, M. F. (2001). Effective properties of the octet-truss lattice material. Journal of the Mechanics and Physics of Solids, 49(8), 1747-1769.

[27] Amani, Y., Dancette, S., Delroisse, P., Simar, A., & Maire, E. (2018). Compression behavior of lattice structures produced by selective laser melting: X-ray tomography based experimental and finite element approaches. Acta Materialia, 159, 395-407.

[28] Hamilton, K. (2016). Planning, preparing and producing: Walking the tightrope between additive and subtractive manufacturing. Metal AM, 2(1), 39-56.

[29] Xu, S., Shen, J., Zhou, S., Huang, X., & Xie, Y. M. (2016). Design of lattice structures with controlled anisotropy. Materials & Design, 93, 443-447.

[30] Moufki, A., Dudzinski, D., & Le Coz, G. (2015). Prediction of cutting forces from an analytical model of oblique cutting, application to peripheral milling of Ti-6Al-4V alloy. The International Journal of Advanced Manufacturing Technology, 81(1-4), 615-626.

[31] Moufki, A., Dudzinski, D., Molinari, A., & Rausch, M. (2000). Thermoviscoplastic modelling of oblique cutting: forces and chip flow predictions. International Journal of Mechanical Sciences, 42(6), 1205-1232.